

Destabilization of a Viscous Film Flowing Down in the Form of a Vertical Cylindrical Curtain

Christophe Pirat,^{1,2} Christian Mathis,¹ Manoranjan Mishra,¹ and Philippe Maïssa^{1,*}

¹*Institut Non Linéaire de Nice, UMR CNRS 6618, Université de Nice-Sophia Antipolis,
1361 Route des Lucioles, F-06560 Valbonne, France*

²*Department of Applied Physics, University of Twente, 7500 AE Enschede, The Netherlands*

(Received 3 February 2006; published 1 November 2006)

In this Letter, we study experimentally a viscous liquid curtain in an annular geometry. Gap and median radius can be varied in such a way that the base of the initially stationary cylindrical curtain is led to oscillate by decreasing the flow rate. Standing and traveling waves in the plane of the annulus are observed and a nontrivial expression linking pulsation to flow rate per surface unit and viscosity can be defined.

DOI: [10.1103/PhysRevLett.97.184501](https://doi.org/10.1103/PhysRevLett.97.184501)

PACS numbers: 47.20.Dr, 47.55.nm, 68.15.+e, 68.18.Jk

Since early studies of Savart [1] and Boussinesq [2], numerous investigations have focused on the formation and stability of liquid curtains [3–6], which are of some importance for coating techniques, both from fundamental and practical points of view. In most experiments, sheets are obtained by a flow through a slot which induces a jet at its outlet, with slot geometry allowing various sheet shapes [3,7–9]. In his experimental work, Brown [3] suggested that curtain stability is related to a minimal strength of the flow rate with the inertial effects overcoming the capillary ones and preventing a transient hole from propagating upstream and eventually destroying the sheet. Another experiment [10], using an overflowing circular dish, leads to a jet with asymmetrical boundary conditions at its very beginning and is directed toward bell shapes. Other investigations [5] are concerned with surface wave effects that appear and propagate along a sheet, in the form of varicose and sinuous waves. In addition, Giorgiutti *et al.* [11] experimented with overflow through a longitudinal slot at the top of a horizontal cylinder, leading to a linear film at the base where the boundary is not constrained in a transverse direction. This gives rise to a chessboard wave pattern.

The present study departs from the previous approaches cited above by adapting the two-dimensional (2D) experimental setup used previously to investigate the destabilization of a liquid film [12]. The current research, in a lower dimensionality, analyses the spatiotemporal behavior of a film in sheet regime. In this case, the liquid does not pass through a slot but through a grid which enables the formation of a liquid film underneath. An annulus with variable radius and gap is used, so that the sheet resulting from the destabilization of the continuously fed film can move freely underneath this surface of variable dimension. Whereas the curtain remains fixed to the base plate in [10], the system presented here uses another degree of freedom—the gap Δ . Experiments have been conducted starting from the destabilization of a well-controlled stationary cylindrical curtain to study the behavior of the resulting dynamical system. A sheet flowing down in such specific boundary conditions shows hitherto unrecognized modes of spontaneous oscillation.

The apparatus employed consists of a circular grid which is used as a porous medium and fixed horizontally at the bottom of a transparent cylindrical tank filled from above with a viscous liquid [Fig. 1(a)]. The annular flow area is obtained using different masks placed on the grid [Fig. 1(b)]. A constant and controlled depression is kept in the tank in order to maintain a fixed and sufficient height of fluid above the grid (about 10 cm). When the device is not fed, the system is at rest. In other words, there is no flow. Flow rate Q is controlled with a valve and measured with a flowmeter. In this way, any incoming fluid flows through the whole annulus and a uniform laminar film is formed below it. As in the 2D case [12], the steel grid is 1 mm in thickness, with circular holes of 1 mm in diameter arranged on a 2 mm regular, hexagonal lattice. The ability to change annulus width, by varying the radius of the inner and outer masks, is one of the novelties of this experimental setup. The present results have been obtained with four gaps (Δ) of 10, 12, 14, and 16 mm, respectively, and with a median radius $r = 56$ mm [Fig. 1(b)]. The viscous liquid is silicone oil with a surface tension $\gamma = 20.6$ dyn/cm, a density $\rho = 0.97$ g/cm³, and three different viscosities $\nu = 200, 100,$ and 50 mm²/s.

Observations are made from above, through the grid, with a digital camera connected to a computer for video capture and processing. Pattern outline is detected by using the refractive properties of the oil, thanks to a peripheral

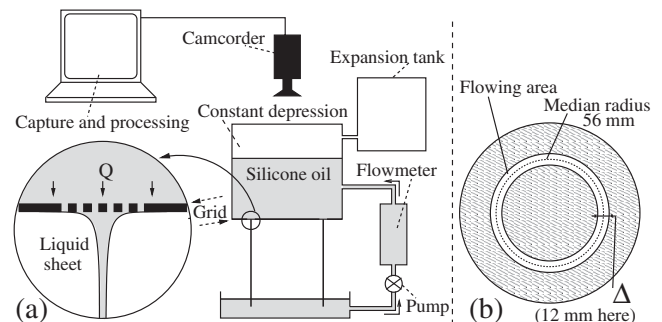


FIG. 1. Schematic drawing of (a) the setup and (b) the flow area.

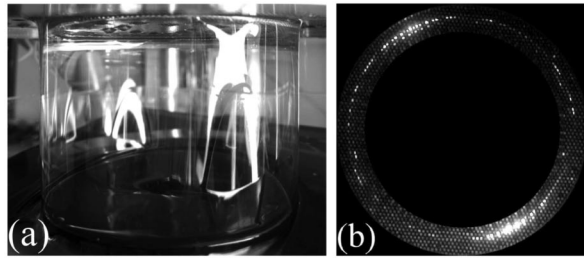


FIG. 2. Cylindrical curtain of silicone oil: (a) side view and (b) from above, through the grid ($\nu = 50 \text{ mm}^2/\text{s}$).

oblique illumination. As the bright zone corresponds to a local increase in film thickness, any draw down area is revealed at the base and appears as a contrasting pattern [see Figs. 2(b) and 3].

If the flow rate is high enough, a closed and stationary liquid curtain can take place. In this instance, it is never cylindrical but tends to close up downstream. It is relevant to note concerning sheets obtained below an overflowing circular dish, which Brunet *et al.* [10] have shown that the curvature—that is, the shape—of the bell automatically adjusts as the flow rate is changed. In our case, in order to carry out a controlled study, a cylindrical curtain [Fig. 2] is generated using a low pressure, one-off inflationary impulse with a small wettable tube (3 mm outer diameter) through its wall. It should be noted that this process neither breaks the curtain nor propagates perturbations upward, which shows the great stability of this kind of curtain to disturbances. This cylindrical curtain becomes centered in the annular area such that its attachments to the film (basal inner and outer interfaces) are almost symmetrical [Fig. 4(a)]. Moreover, its translation invariance in the vertical direction (flow direction) is no more sensitive to flow rate changes. By contrast a noncylindrical curtain does not exhibit such interesting properties.

The continuously fed film behavior is similar to the one observed in the 2D case [12] where liquid columns and sheets are successively obtained at increasing flow rates. So we clearly observe in the present experiment a

Rayleigh-Taylor-type instability. In the columns, regime emitting sites form a 1D cellular pattern with a wavelength close to $\lambda_{\text{RT}} = 2\pi\sqrt{2}l_c = 13.3 \text{ mm}$ with a capillary length $l_c = \sqrt{\gamma/\rho g}$ [Fig. 3(a)]. In this connection, previous studies [11–13] have reported that column oscillations are a generic response in this regime. Indeed, radial oscillations of curtain base, primarily induced by competition between gravity and surface tension, are actually observed only for values of Δ near λ_{RT} , chosen as a reference gap.

The following scenario holds for all the viscosities and gaps we used. By decreasing slowly the flow rate, starting from the stationary state [Fig. 4(a)], the film and the cylindrical curtain get thinner [Fig. 4(b)]. At some critical flow rate Q_c the curtain begins to oscillate radially [Figs. 4(c)–4(g)] and a standing wave (SW, wave number κ_M , pulsation ω_M) develops. In the film plane, this one can be described as a combination of two counterpropagating traveling waves (TWs, left and right) of equal amplitude. We confirmed that, at first order, observed oscillations are sinusoidal ones. For decreasing values below the Q_c threshold, oscillation amplitude increases and pulsation decreases. At a lower flow rate, a second transition occurs. The system selects the left or the right TW matching the same wave number κ_M —the maximum value allowed for a given couple (Δ , ν)—and the current value of the pulsation of the SW. Once again by decreasing the flow rate the pulsation ω decreases while the amplitude increases until a lower wave number κ is selected by the system. The same behavior can be observed several times while decreasing the flow rate until the curtain breaks down into columns. By contrast, if the flow rate is increased, the system demonstrates the reverse transitions for a different set of critical flow rate values. It would appear that the SW oscillation is due to a local and periodic film thickness difference in front of and behind the initial stationary curtain. The onset of the TW is due to a second symmetry-breaking when the overthickness of the film in the azimuthal direction is no longer stationary. It is possible to directly obtain a TW by choosing a flow rate which selects a given wave number κ . We adopt a normalized wave number $N = \kappa \cdot r$ and, for

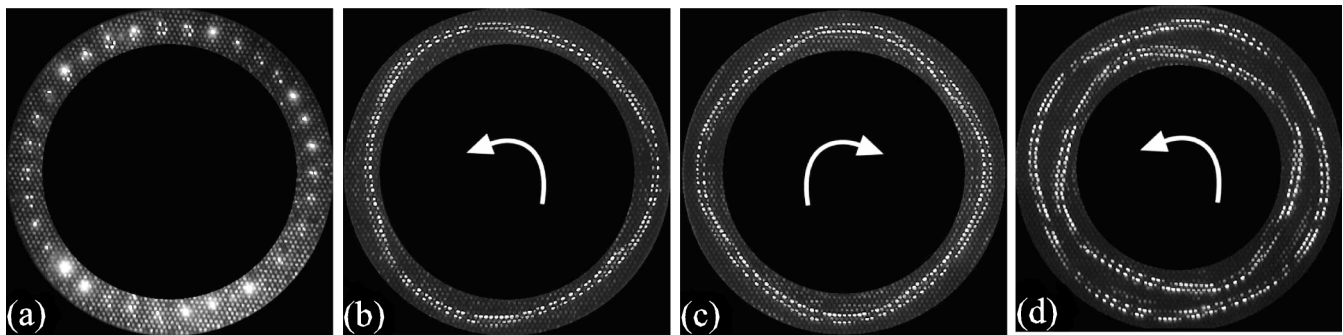


FIG. 3. (a) 1D cellular pattern of liquid columns ($\Delta = 14 \text{ mm}$); (b),(c) traveling waves seen from above, (b) $N = 3$, $\Delta = 14 \text{ mm}$, and (c) $N = 4$, $\Delta = 16 \text{ mm}$ ($\nu = 200 \text{ mm}^2/\text{s}$ and $r = 56 \text{ mm}$). (d) A more complicated case: two distinct corotating curtains (separated by an air layer, $r = 52 \text{ mm}$, $\Delta = 24 \text{ mm}$, $\nu = 50 \text{ mm}^2/\text{s}$).

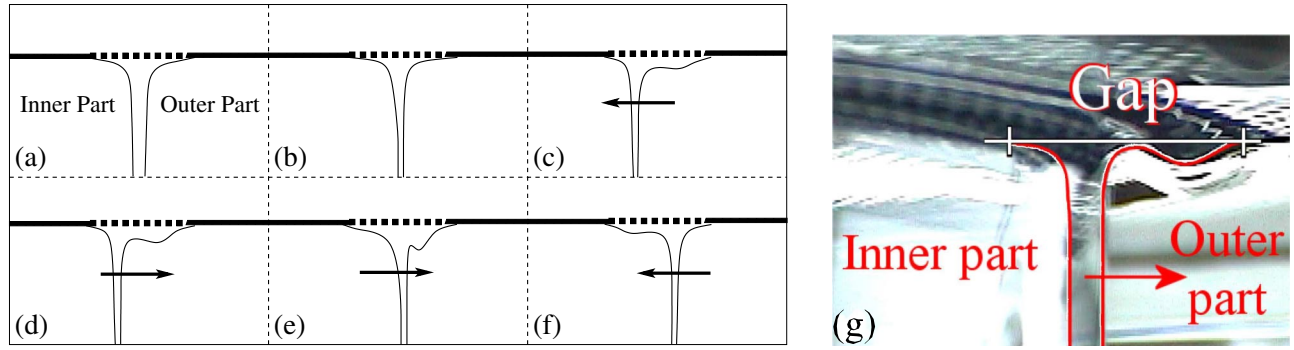


FIG. 4 (color online). Schematic evolution of the curtain cross section: (a) the flow rate is larger than Q_c and the curtain is thick and stationary; (b) at decreasing flow rate, the curtain gets thinner; (c)–(f) for a flow rate lower than or equal to Q_c the original curtain base present at the outset destabilizes and oscillates. (g) Snapshot corresponding to (d).

the sake of clarity, set the angular velocity as $\Omega = \frac{1}{r} \left(\frac{d\theta}{dt} \right)$. The curtain base can be also seen as a rotating regular “polygonal” pattern [Figs. 3(b) and 3(c)].

In the chosen range of Δ values, we have obtained N values of between 1 and 4, 1 and 6, and 1 and 8, respectively, for 200, 100, and 50 mm^2/s viscosity oils. As soon as a given value of N is selected by the system, this solution persists for a range of flow rate values and Ω evolves linearly with the flow rate. Figure 5 depicts this evolution for the four Δ values with $\nu = 200 \text{ mm}^2/\text{s}$. The larger the values of Δ , the greater the N values selected by the system. A given N value can be found with different Δ but with a change of associated Ω . All the results can be represented as a single curve if one considers ω as a function of the flow rate per surface unit U_0 (average velocity of the fluid through the grid), as is shown in Figs. 6(a)–6(c), respectively, for the 200, 100, and 50 mm^2/s viscosity oils. The higher the viscosity, the smaller the dispersion. The minimal flow rate before the curtain breaks down into columns is a function of viscosity and Δ . The median radius r , which is a constant here, plays also a role but does not change the global qualitative behavior. There is no simple criterion based on a Weber number to characterize curtain stability as described in other studies [5,6,9,10]. Our system is not concerned with upstream perturbations but with another type of instability as discussed above. Actually, there is competition between two stationary states for the range of studied flow rates: a periodic pattern of liquid columns and an oscillating cylindrical sheet.

It should be pointed out that if the gap Δ is too small (less than $0.75\lambda_{RT}$), there is no destabilization of the curtain. For these small gaps only, the structures and dynamics are similar to those studied previously in other experiments [11,13]. If Δ is larger than $1.25\lambda_{RT}$, the system exhibits more complicated patterns which are of interest but beyond the scope of the present study [see an example in Fig. 3(d)]. Solutions depart from quasi-1D behaviors.

We propose here a qualitative explanation for the average evolution of ω vs U_0 by considering its viscosity dependence. From experimental data in Figs. 6(a)–6(c) we expect that the relation between pulsation and average velocity could be roughly expressed as

$$\omega = aU_0/l^* + b, \quad (1)$$

where a and b are constants and l^* is a characteristic length.

Using a dimensional approach taking into account ν , g , and, to describe the behavior of the curtain near its base, Q , we get $l^* = (Q\nu g^{-1})^{1/4}$ as a characteristic length valid near the sheet base. Both viscosity and flow rate dependences are equally considered. Clarke [8] has introduced the same characteristic length to describe, near the orifice, a sheet falling from a slot. Equation (1) then becomes $\omega = aU_0/(Q\nu g^{-1})^{1/4} + b$. Since $Q \propto U_0$, one gets

$$\omega = a'U_0^{3/4} + b, \quad (2)$$

where

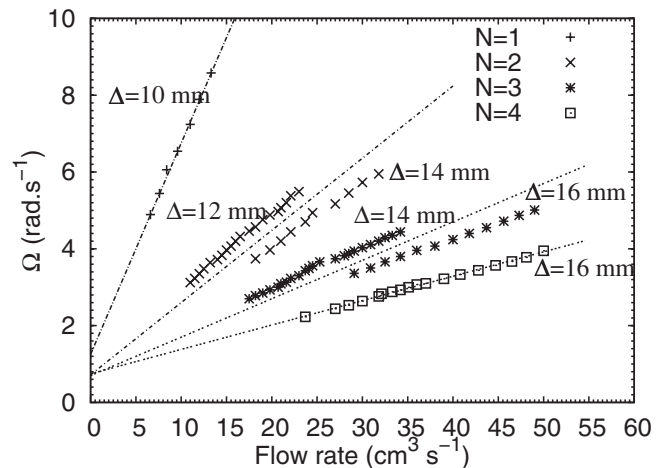


FIG. 5. Angular velocity Ω vs flow rate, $r = 56 \text{ mm}$, $\Delta = 10, 12, 14, \text{ and } 16 \text{ mm}$ ($\nu = 200 \text{ mm}^2/\text{s}$).

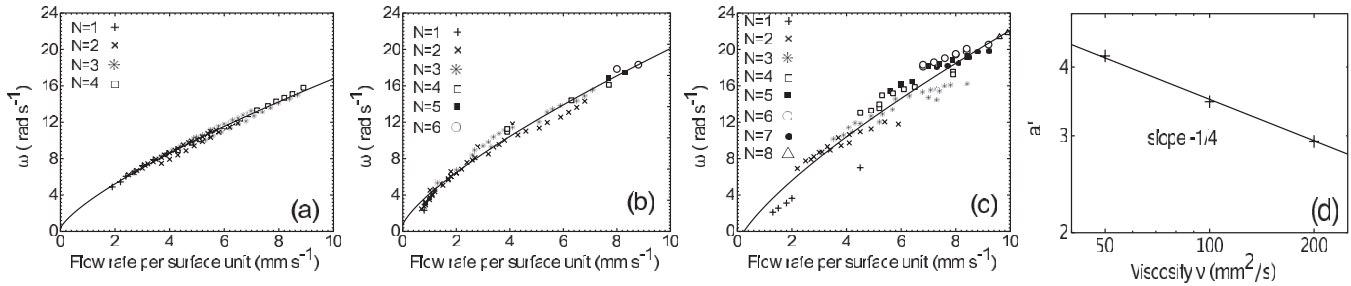


FIG. 6. Pulsation ω vs flow rate per surface unit for ν equal to (a) 200, (b) 100, and (c) 50 mm^2/s . The curve fittings correspond to Eq. (2). (d) Curve fitting of the viscosity dependence of a' using Eq. (3) (log-log plot).

$$a' = a''/\nu^{1/4}, \quad (3)$$

a'' being a constant of proportionality. The experimental data of ω vs U_0 for different viscosities ($\nu = 200, 100,$ and $50 \text{ mm}^2/\text{s}$) are well fitted with Eq. (2), and the resulting curves are presented in Figs. 6(a)–6(c). The validity of the associated power-law relationship (3) is confirmed, as shown in Fig. 6(d), in a log-log plot, giving the viscosity dependence of a' values obtained previously.

The dynamics of a viscous film in a specific down flow configuration in the sheet regime—the cylindrical curtain—is revealed in this study. We show for the first time the existence of spontaneous standing and traveling waves resulting from radial oscillations in the film plane itself, i.e., where the curtain originates. We have demonstrated a range of normalized wave numbers N for each couple (Δ, ν). Focusing on the traveling wave case and for a given N , the angular velocity Ω is proportional to the flow rate. We have also shown that the influence of viscosity on the average evolution of the pulsation ω is a function of the flow rate per surface unit. We define a characteristic length and propose nontrivial expressions that agree with our experimental results. Such sheet dynamics, not limited by annular geometry, can be carefully controlled and should find their place in potential applications. Our hope is to stimulate further research in this area with this Letter. A more precise description of wave number (N) selection is underway and will appear in a forthcoming publication.

M. M. gratefully acknowledges support from French Ministry of Education and Research. We also thank Jean-Charles Bery for his technical support and invaluable help.

*Electronic address: Philippe.Maissa@inln.cnrs.fr

- [1] F. Savart, Ann. Chim. (Paris) **54**, 56 (1833).
- [2] J. Boussinesq, C.R. Acad. Sci. Paris **69**, 45 (1869); **69**, 128 (1869).
- [3] D. R. Brown, J. Fluid Mech. **10**, 297 (1961).
- [4] L. de Luca and M. Costa, Eur. J. Mech. B, Fluids **16**, 75 (1997); J. Fluid Mech. **331**, 127 (1997).
- [5] S. P. Lin and G. Roberts, J. Fluid Mech. **104**, 111 (1981).
- [6] N. Le Grand-Piteira, P. Brunet, L. Lebon, and L. Limat, Phys. Rev. E **74**, 026305 (2006).
- [7] J. I. Ramos, Comput. Theor. Polym. Sci. **11**, 429 (2001).
- [8] N. S. Clarke, J. Fluid Mech. **31**, 481 (1968).
- [9] K. Adachi, J. Non-Newtonian Fluid Mech. **24**, 11 (1987); K. Adachi *et al.*, AIChE J. **36**, 738 (1990).
- [10] P. Brunet, C. Clanet, and L. Limat, Phys. Fluids **16**, 2668 (2004).
- [11] F. Giorgiutti, A. Bleton, L. Limat, and J. E. Wesfreid, Phys. Rev. Lett. **74**, 538 (1995).
- [12] C. Pirat, C. Mathis, P. Maïssa, and L. Gil, Phys. Rev. Lett. **92**, 104501 (2004).
- [13] C. Counillon, L. Daudet, T. Podgorski, and L. Limat, Phys. Rev. Lett. **80**, 2117 (1998).